Supporting Information

Lead(II) Complex Formation with *L*-Cysteine in Aqueous Solution

Farideh Jalilehvand [a,*], *Natalie S. Sisombath* [a], *Adam C. Schell* [a] *and Glenn A. Facey* [b]

[a] Department of Chemistry, University of Calgary, 2500 University Drive NW, Calgary, Alberta T2N 1N4, Canada

[b] Department of Chemistry, University of Ottawa, 10 Marie Curie Private, Ottawa, Ontario, K1N 6N5, Canada

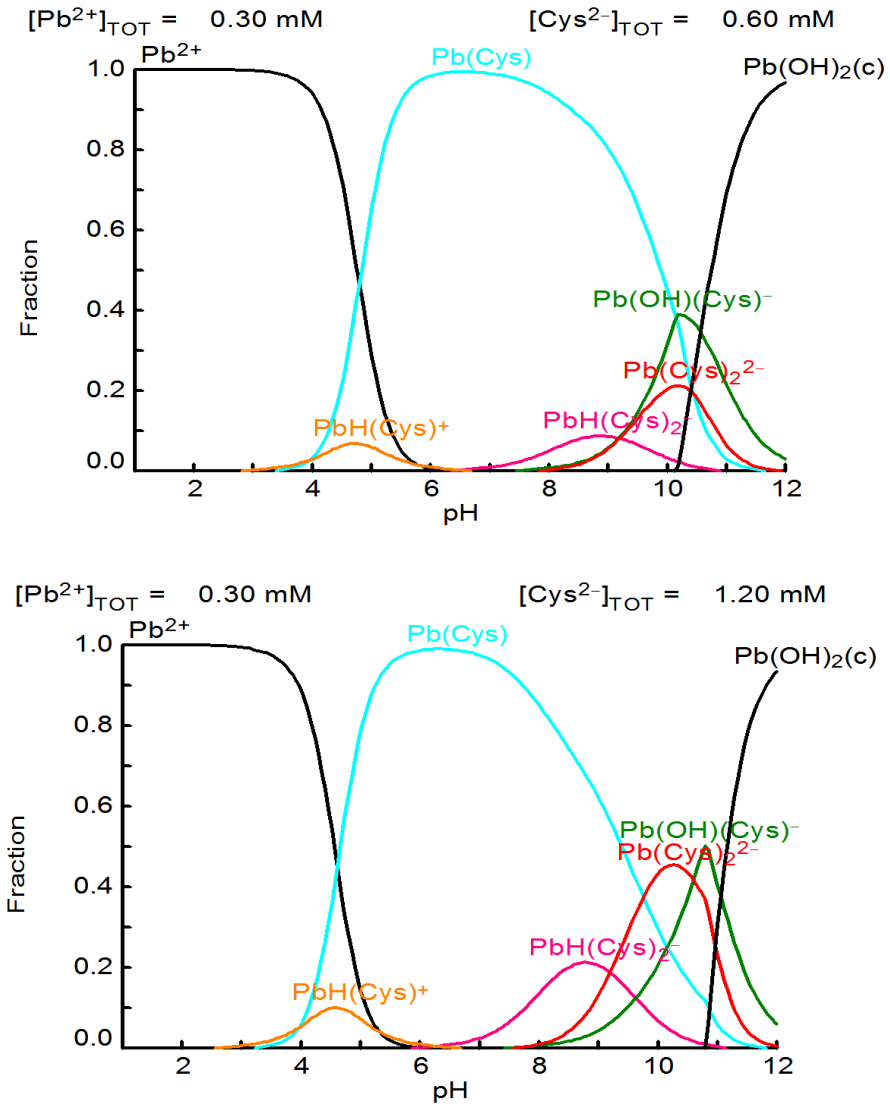

Figure S-1a. Distribution diagrams for lead(II) cysteine complexes as a function of pH in solutions containing $C_{Pb(II)}$ = 0.3 mM and H_2Cys / Pb(II) mole ratios 2.0 and 4.0, based on the reported formation constants by Bizri et al., calculated at 25 ºC in the ionic medium 1.0 M $NaClO_4$ [16] for the following aqueous Pb(II)-cysteine complexes:

$$p\ Pb^{2+} + q\ H^{+} + r\ Cys^{2-} \leftrightarrow Pb_p H_q (Cys)_r \qquad \beta_{p,\,q,\,r}$$

Pb(Cys) (log $\beta_{1,\,0,\,1}$ = 12.2), Pb(Cys)(OH)$^-$ (log $\beta_{1,\,-1,\,1}$ = 2.04), $Pb(Cys)_2^{2-}$ (log $\beta_{1,\,0,\,2}$ = 15.9), Pb(HCys)(Cys)$^-$ (log $\beta_{1,\,1,\,2}$ = 25.10) and Pb(HCys)$^+$ (log $\beta_{1,\,1,\,1}$ = 16.16).

The solid compound PbCys(c) is soluble at such low concentration; however, no solubility product (or formation constant) has been reported.

The distribution diagrams in Figures S-1a were calculated with computer program MEDUSA (http://www.kemi.kth.se/medusa/). The full input file to MEDUSA is:

```
  3,  17,  4,  0   /MEDUSA, t = 25 C, p = 1
Pb 2+
H+
Cys 2-
H(Cys)-          ,   10.19    0  1  1
H2(Cys)          ,   18.44    0  2  1
H3(Cys)+         ,   20.53    0  3  1
OH-              ,  -14.0     0 -1  0
PbH(Cys)+        ,   16.16    1  1  1
PbH(Cys)2 -      ,   25.1     1  1  2
Pb(Cys)          ,   12.2     1  0  1
Pb(Cys)2 2-      ,   15.9     1  0  2
Pb(OH)(Cys)-     ,    2.04    1 -1  1
Pb(OH)2          ,  -17.12    1 -2  0
Pb(OH)3 -        ,  -28.06    1 -3  0
Pb(OH)4 2-       ,  -39.7     1 -4  0
Pb2(OH) 3+       ,   -6.36    2 -1  0
Pb3(OH)4 2+      ,  -23.88    3 -4  0
Pb4(OH)4 4+      ,  -20.88    4 -4  0
Pb6(OH)8 4+      ,  -43.61    6 -8  0
PbOH +           ,   -7.71    1 -1  0
PbCys(c)         ,   15.2     1  0  1
Pb(OH)2(c)       ,   -8.15    1 -2  0
PbO(cr)          ,  -12.91    1 -2  0
PbO:Pb(OH)2(c) ,  -26.2     2 -4  0
Pb 2+,  H+,
T,  0.01
LAV, -1.0   -13.0
T,  0.02
```

Note: The formation constant log β for solid PbCys(c) is an estimated value for this ionic strength (I = 1.0 M). The stability constants for Pb(II) hydroxo complexes (including $Pb(OH)_4^{2-}$) have been introduced from the database HYDRA in MEDUSA program.

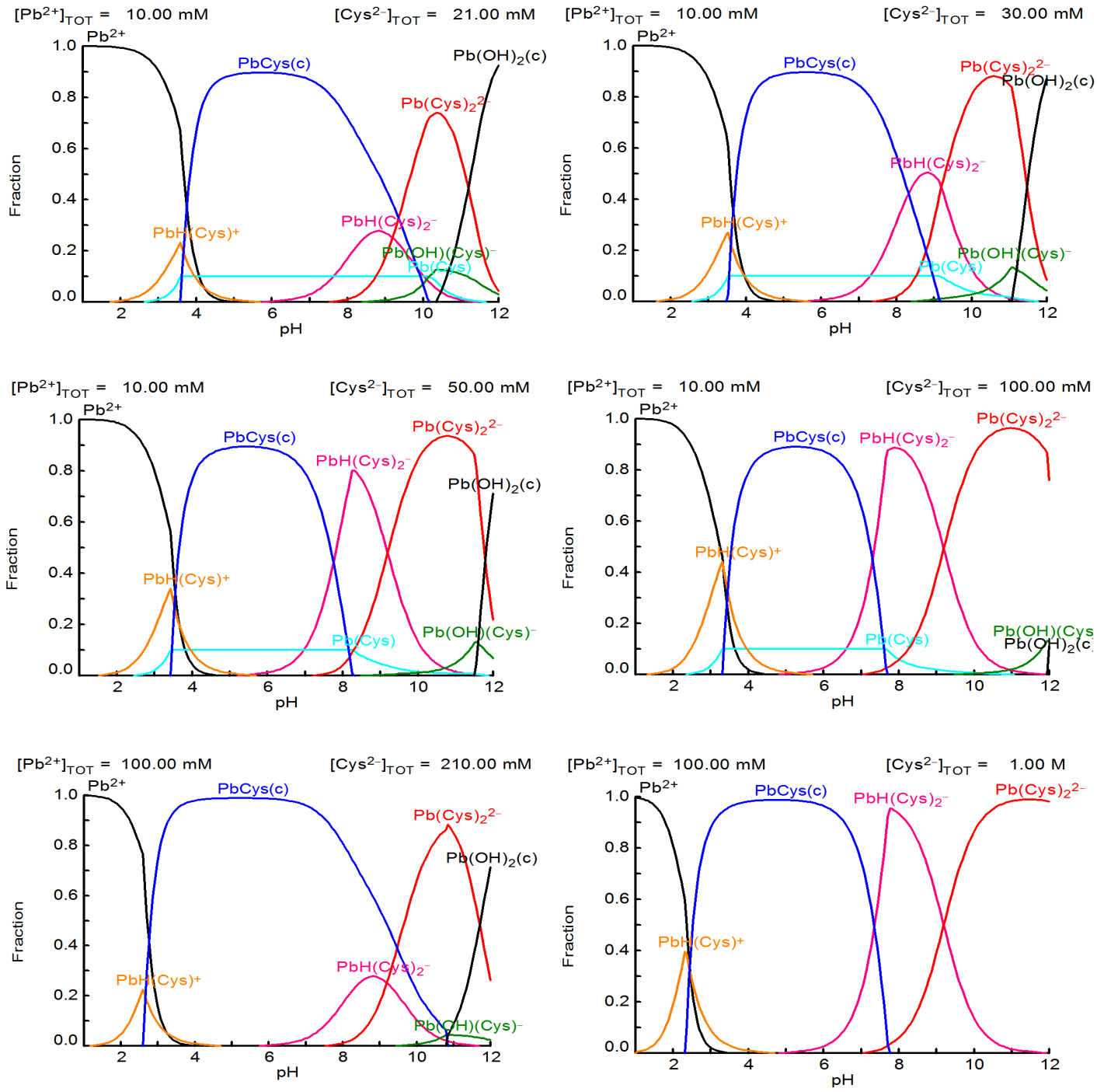

Figure S-1b. Distribution diagrams for lead(II) cysteine complexes as a function of pH in solutions containing $C_{Pb(II)}$ ~ 10 mM or 100 mM, and H_2Cys / Pb(II) mole ratios 2.1, 3.0, 5.0 or 10.0, based on the reported formation constants for I = 1.00 M by Bizri et al. (used in Figure S-1a) [16]. A tentative solubility product of log K_{sp} = -15.2 was estimated for PbCys(c), with formation constant of log β = 15.2, to represent our experimental observations in the current study, i.e. dissolution of the PbCys(c) precipitate at pH = 10.4 in solutions with H_2Cys/Pb(II) mole ratio 2.1 (A and A*), and at pH ≤ 9.1 for those with higher H_2Cys/ Pb(II) mole ratios.

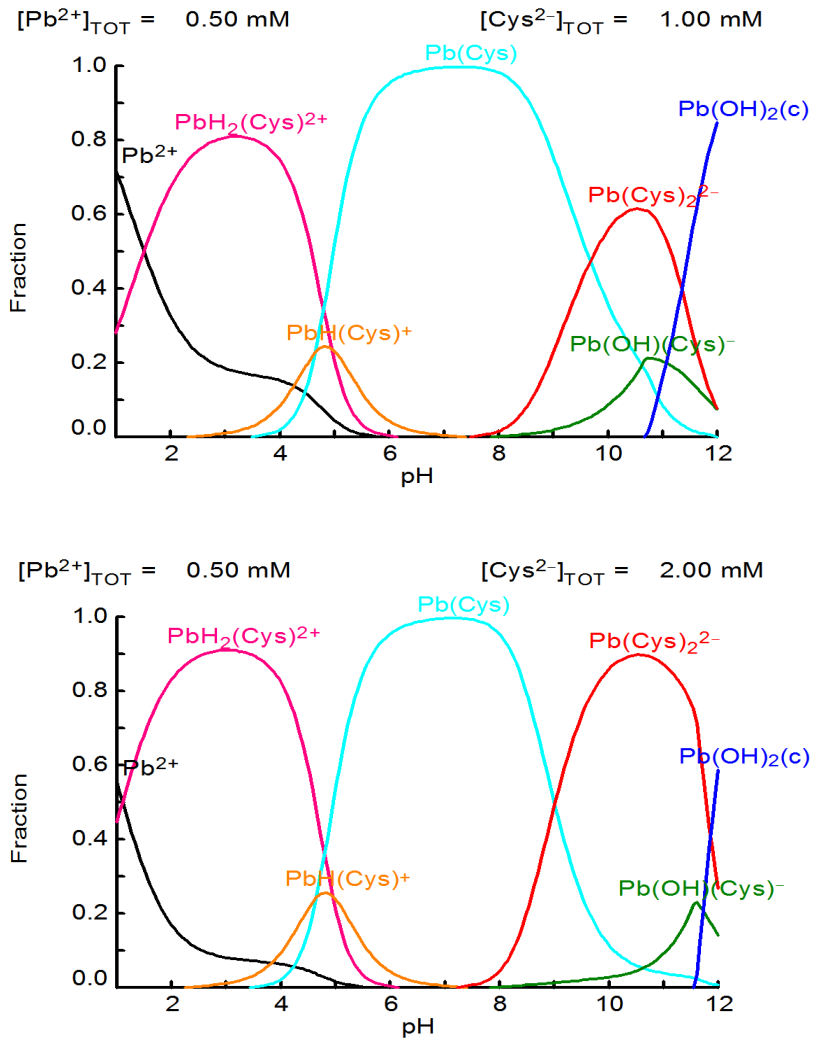

Figure S-2a. Distribution diagrams for lead(II) cysteine complexes as a function of pH in solutions containing $C_{Pb(II)}$ = 0.5 mM and H_2Cys / Pb(II) mole ratios 2.0 and 4.0, based on the reported formation constants by Crea et al., calculated at 25 ºC in the ionic medium 0.1 M $NaNO_3$ [20] for the following aqueous Pb(II)-cysteine complexes:

$$p\ Pb^{2+} + q\ H^{+} + r\ Cys^{2-} \leftrightarrow Pb_p H_q (Cys)_r \qquad \beta_{p,\,q,\,r}$$

$Pb(Cys)$ ($\log \beta_{1,\,0,\,1} = 13.12$), $Pb(Cys)(OH)^-$ ($\log \beta_{1,\,-1,\,1} = 2.49$), $Pb(Cys)_2^{2-}$ ($\log \beta_{1,\,0,\,2} = 17.56$), $Pb(H_2Cys)^{2+}$ ($\log \beta_{1,\,2,\,1} = 22.72$) and $Pb(HCys)^{+}$ ($\log \beta_{1,\,1,\,1} = 17.77$).

The distribution diagrams in Figure S-2a were calculated with computer program MEDUSA (http://www.kemi.kth.se/medusa/). The full input file to MEDUSA is:

```
  3,  16,  4,  0   /MEDUSA, t= 25 C, p= 1
Pb 2+
H+
Cys 2-
H(Cys)-            ,   10.46    0  1  1
H2(Cys)            ,   18.78    0  2  1
H3(Cys)+           ,   21.04    0  3  1
OH-                ,  -14.0     0 -1  0
Pb(Cys)            ,   13.12    1  0  1
PbH(Cys)+          ,   17.77    1  1  1
PbH2(Cys) 2+       ,   22.72    1  2  1
Pb(Cys)2 2-        ,   17.56    1  0  2
Pb(OH)(Cys)-       ,    2.49    1 -1  1
Pb(OH)2            ,  -17.14    1 -2  0
Pb(OH)3 -          ,  -28.06    1 -3  0
Pb2(OH) 3+         ,   -7.08    2 -1  0
Pb3(OH)4 2+        ,  -23.41    3 -4  0
Pb4(OH)4 4+        ,  -20.13    4 -4  0
Pb6(OH)8 4+        ,  -42.86    6 -8  0
PbOH+              ,   -7.67    1 -1  0
Pb(Cys)(c)         ,    16.2    1  0  1
Pb(OH)2(c)         ,   -8.15    1 -2  0
PbO(cr)            ,  -12.91    1 -2  0
PbO:Pb(OH)2(c)     ,  -26.2     2 -4  0
Pb 2+,  H+,
T,  0.1
LAV, -1.0   -13.0
T,  1.0
```

Note: The formation constant log β for solid PbCys(c) is an estimated value for this ionic strength (I = 0.1 M). The stability constants for Pb(II) hydroxo complexes have been adopted from Table 2 of Crea et al. [20], referring to *Pure Appl. Chem.,* **2009**,*81*, 2425–2476, and do not include the $Pb(OH)_4^{2-}$ complex.

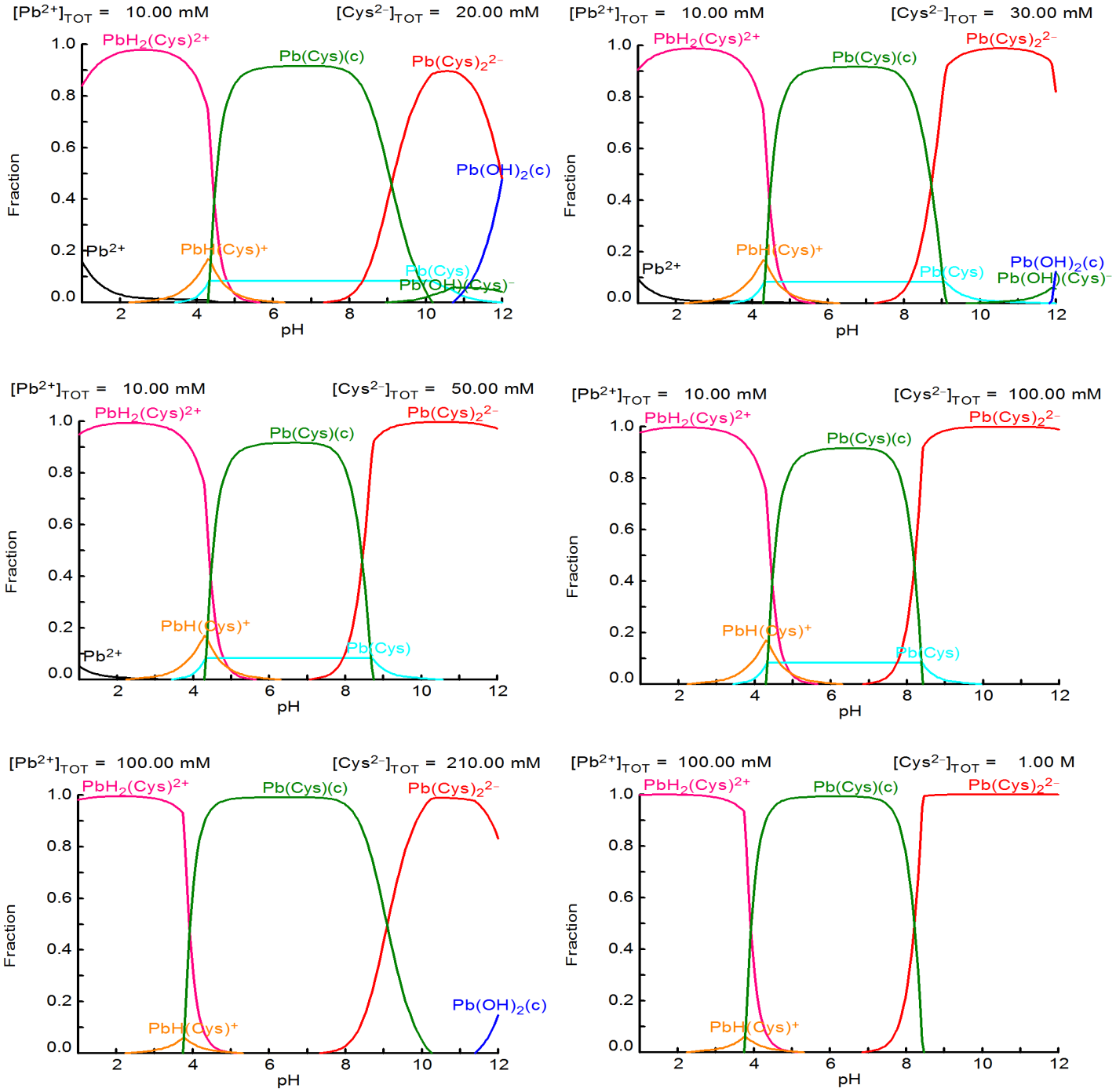

Figure S-2b. Distribution diagrams for lead(II) cysteine complexes as a function of pH in solutions containing $C_{Pb(II)}$ ~ 10 mM or 100 mM, and H_2Cys / Pb(II) mole ratios 2.1, 3.0, 5.0 or 10.0, based on the reported formation constants for I = 0.1 M by Crea et al. (used in Figure S-2a) [20]. A tentative solubility product of log K_{sp} = -16.2 was estimated for PbCys(c), with the formation constant log β = 16.2, to represent our experimental observations in the current study, i.e. dissolution of PbCys(c) precipitate at pH = 10.4 in solutions with H_2Cys/Pb(II) mole ratio 2.1 (A and A*), and at pH $\leq$ 9.1 for those with higher H_2Cys/ Pb(II) mole ratios.

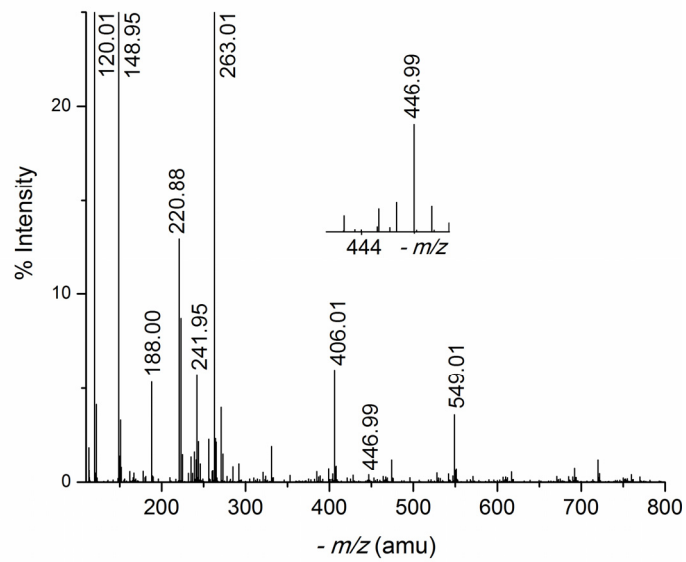

Figure S-3. ESI-MS spectrum in negative ion modes for the alkaline Pb(II)-cysteine aqueous solution F, containing $C_{Pb(II)}$ = 10 mM and C_{H2Cys} = 100 mM, pH = 9.1. The peaks with 100% relative intensity is at *m/z* = 120.01, assigned to $[H_2Cys - H^+]^-$ mass ions (see Table S-1 for peak assignment).

Table S-1. Assignment of mass ions observed in ESI-MS spectra (- mode) for Pb(II)-cysteine solutions A, B and F ($C_{Pb(II)}$ = 10 mM). [a]

m/z (amu)	assignment
120.01	$[H_2Cys - H^+]^-$
220.88	$[Na^+ + 2ClO_4^-]^-$
241.95	$[H_2Cys – H^+ + NaClO_4]^-$
263.01	$[Na^+ + 2H_2Cys – 2H^+]^-$
406.01	$[2Na^+ + 3H_2Cys – 3H^+]^-$
446.99	$[Pb(H_2Cys)_2 – 3H^+]^-$
549.01	$[3Na^+ + 4(H_2Cys) – 4H^+]^-$

[a] H_2Cys ($C_3H_7NO_2S$); *m* = 121.02

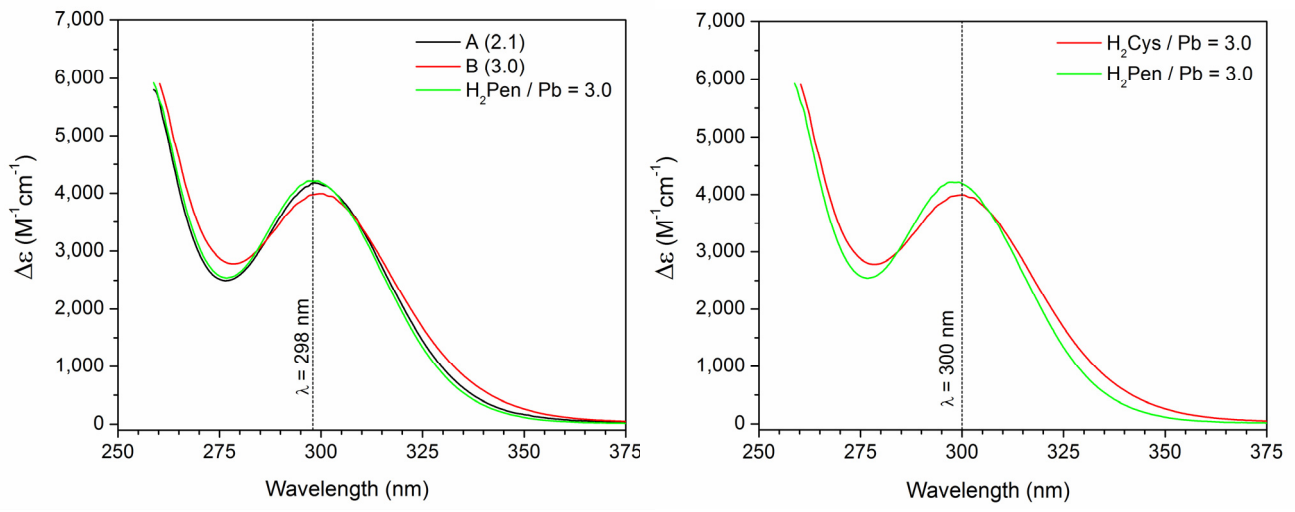

Figure S-4a. UV-vis. spectra of the alkaline aqueous Pb(II) cysteine solutions A (pH = 10.4) and B (pH = 9.1) with $C_{Pb(II)}$ = 10 mM and H_2Cys/ Pb(II) mole ratios 2.1 and 3.0, respectively, compared with that of a Pb(II) penicillamine solution with $C_{Pb(II)}$ = 10 mM and C_{H_2Pen} = 30 mM (pH = 9.6) [26]. The shift in λ_{max} is indicated by the vertical lines.

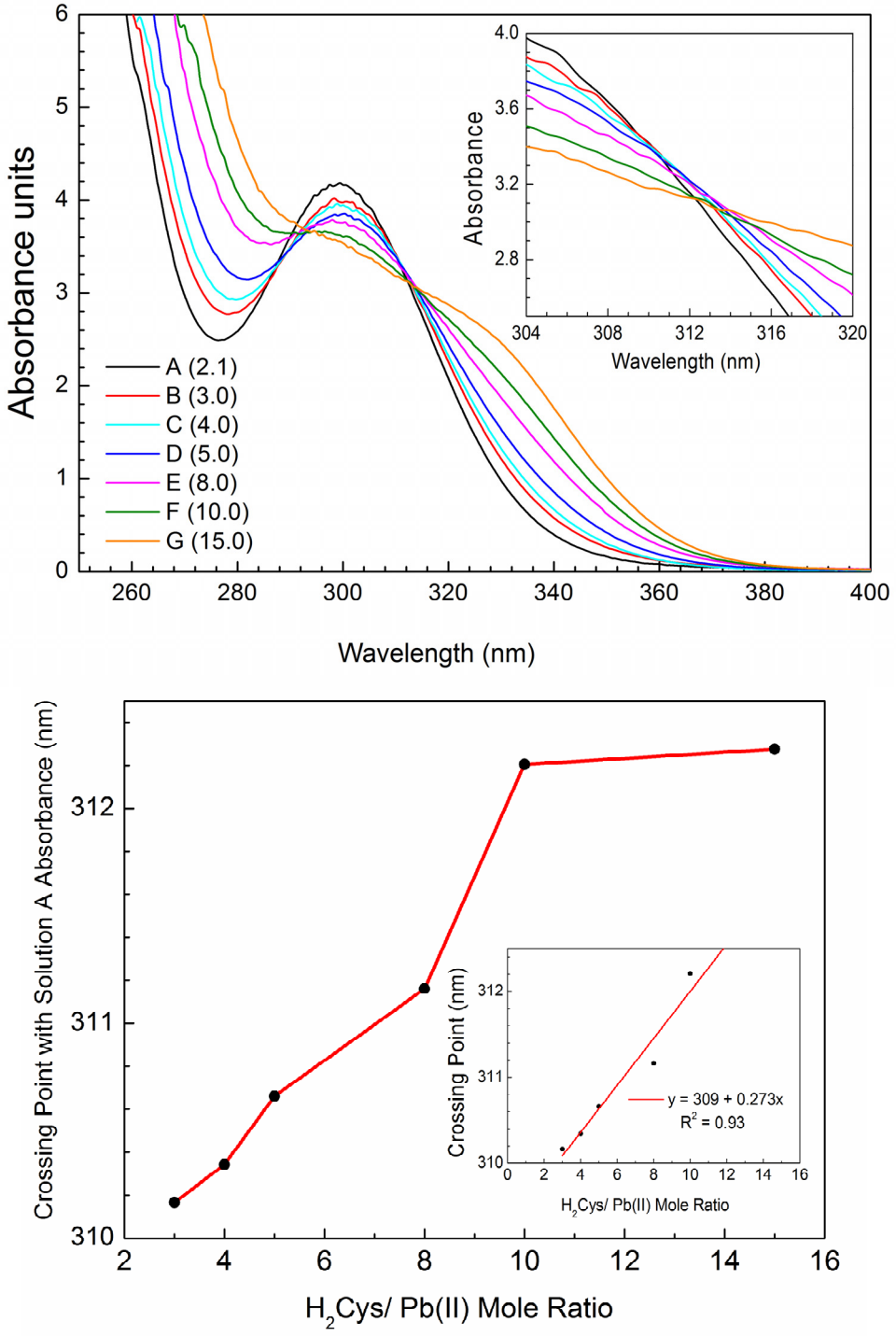

Figure S-4b. (*Top*) UV-vis. spectra of the Pb(II) cysteine solutions A – G (data interval = 0.5 nm), with a close up around 312 nm in inset, showing a systematic movement of the crossing points, spectrum by spectrum. (*Below*) Wavelengths at which the UV-vis. spectra of solutions B – G cross the absorption spectrum of solution A (inset: linear fit to the points corresponding to H_2Cys/Pb(II) mole ratios 3 – 10).

Table S-2. *(Left)* Comparing the difference in ^{13}C NMR chemical shifts ($\Delta\delta$) for Pb(II)-cysteine solutions A – F ($C_{Pb(II)}$ = 10 mM) and free cysteine (pH = 9.1); (*right*) ^{1}H NMR chemical shifts (δ_H) for these solutions (see Figure 3)

Solution	$\Delta\delta$ (^{13}C, ppm)		
	C_1	C_2	C_3
A	5.0	4.1	4.4
B	1.4	1.8	2.0
C	1.4	1.7	2.0
D	1.0	1.3	1.5
E	0.4	0.6	0.9
F	0.2	0.4	0.7

Solution	δ (^{1}H, ppm)		
	H_c	H_a	H_b
$Cys^{2-}/HCys^{-}$	3.63	3.00	2.85
A	4.10	3.66	3.50
B	4.07	3.53	3.45
C	3.94	3.42	3.31
D	3.87	3.34	3.23
E	3.80	3.25	3.12
F	3.76	3.14	3.07

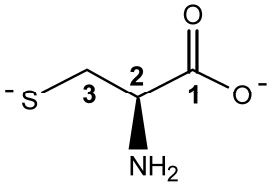

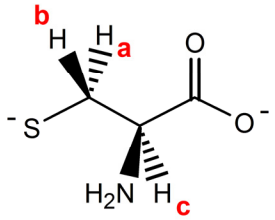

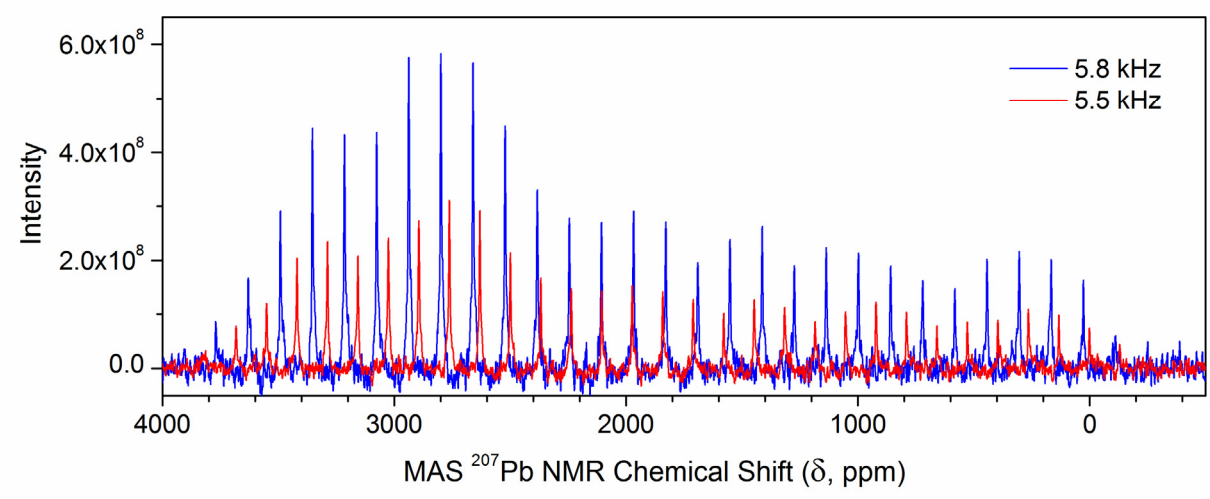

Figure S-5a. Overlapping MAS ^{207}Pb NMR spectra of crystalline Pb(*S,N*-aet)$_2$ measured at MAS rates 5.5 and 5.8 kHz. The isotropic chemical shift is δ_{iso} = 2105 ppm.

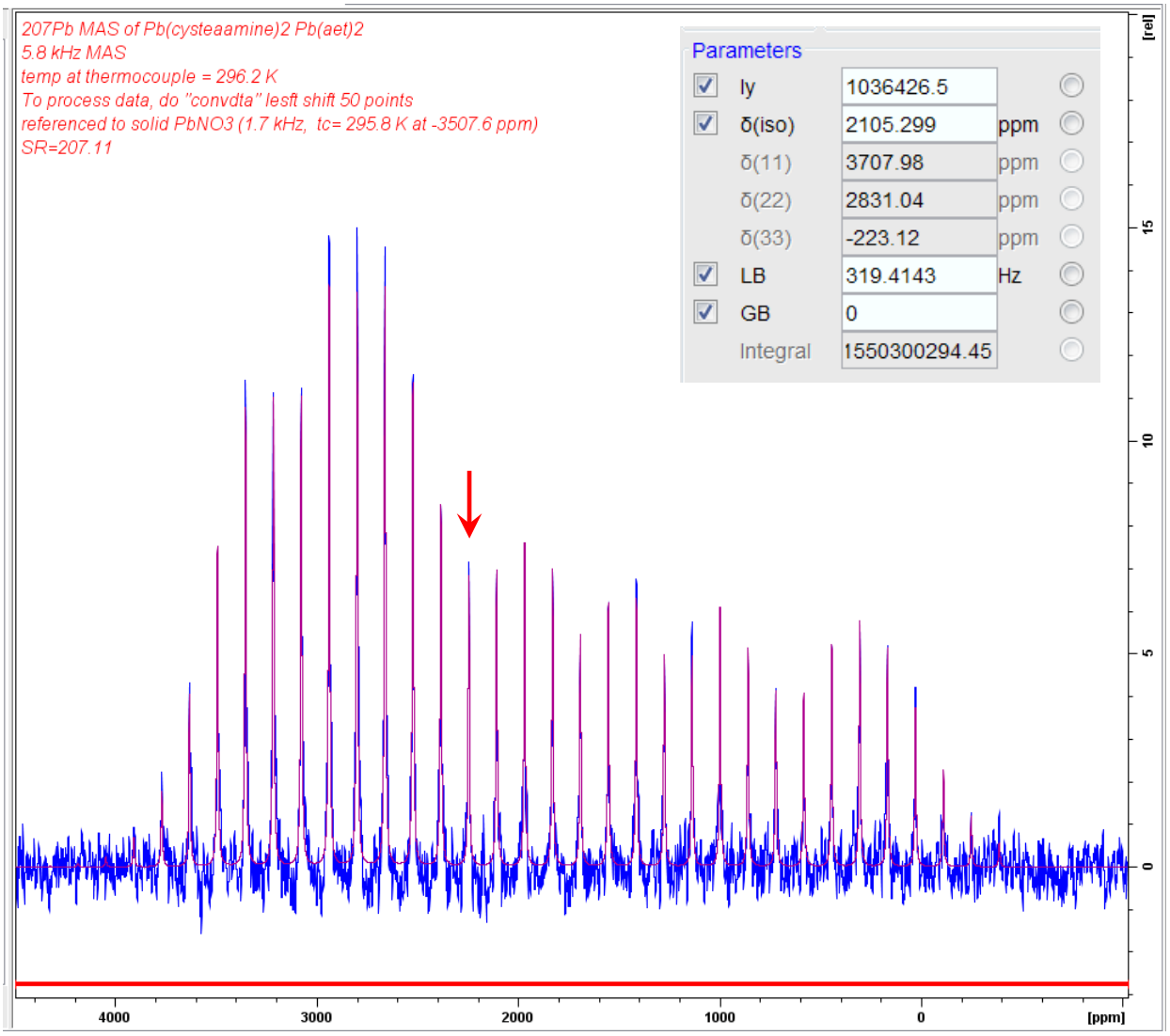

Figure S-5b. One-pulse solid state MAS ^{207}Pb NMR spectrum of crystalline Pb(aet)$_2$ (spinning at 5.8 kHz; blue), and the reconstructed static ^{207}Pb NMR powder pattern (pink). The isotropic chemical shift (δ_{iso} = 2105 ppm) is shown by an arrow.

δ_{11} = 3707.98 ppm; δ_{22} = 2831.04 ppm; δ_{33} = -223.12 ppm;

δ_{iso} = 1/3 (δ_{11} + δ_{22} + δ_{33}) = 2105.3 ppm

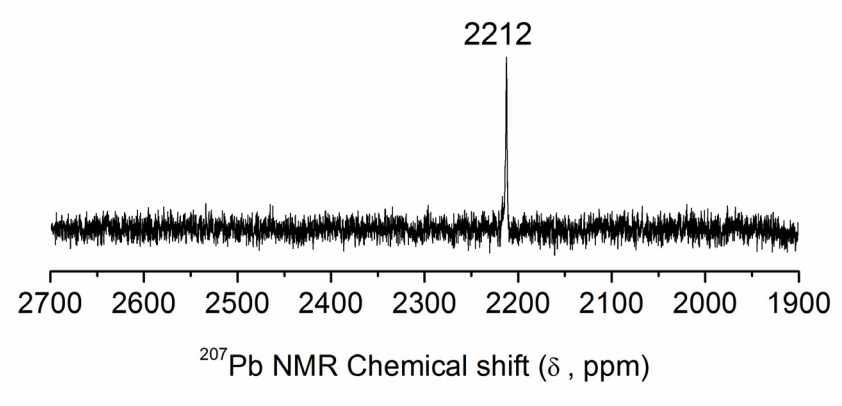

Figure S-6. ^{207}Pb NMR spectrum of an aqueous solution with a Pb(II):cysteamine mole ratio 1:3 (10% D_2O, pH = 10.1, $C_{Pb(II)}$ = 76 mM) prepared by dissolving Pb(*S,N*-aet)$_2$ in a solution containing the same number of Haet moles.

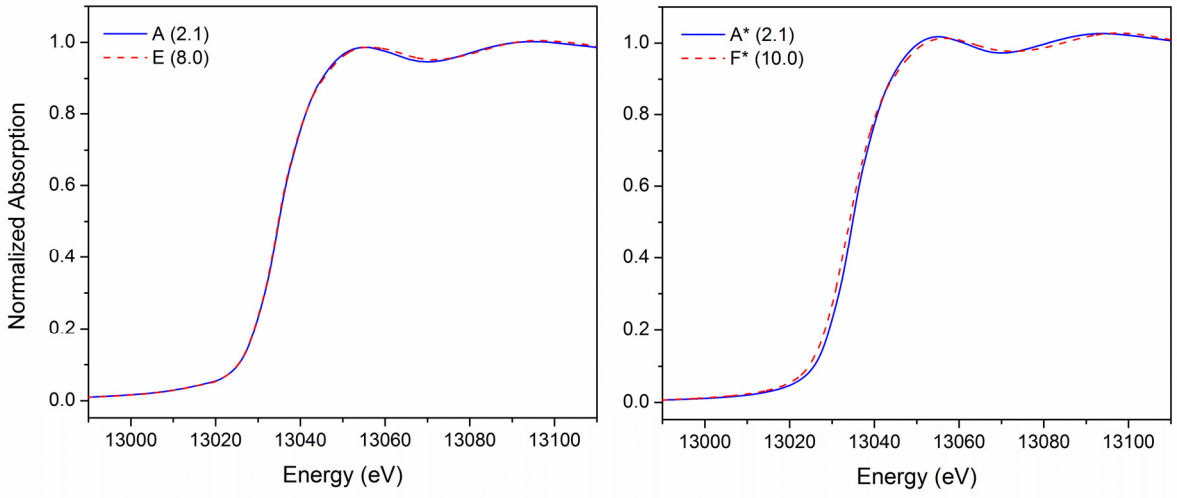

Figure S-7. Pb L_{III}-edge XANES spectra compared for Pb(II)-cysteine alkaline solutions A and E ($C_{Pb(II)}$ = 10 mM), and for solutions A* and F* ($C_{Pb(II)}$ = 100 mM). The H_2Cys/Pb(II) mole ratios are shown in brackets.

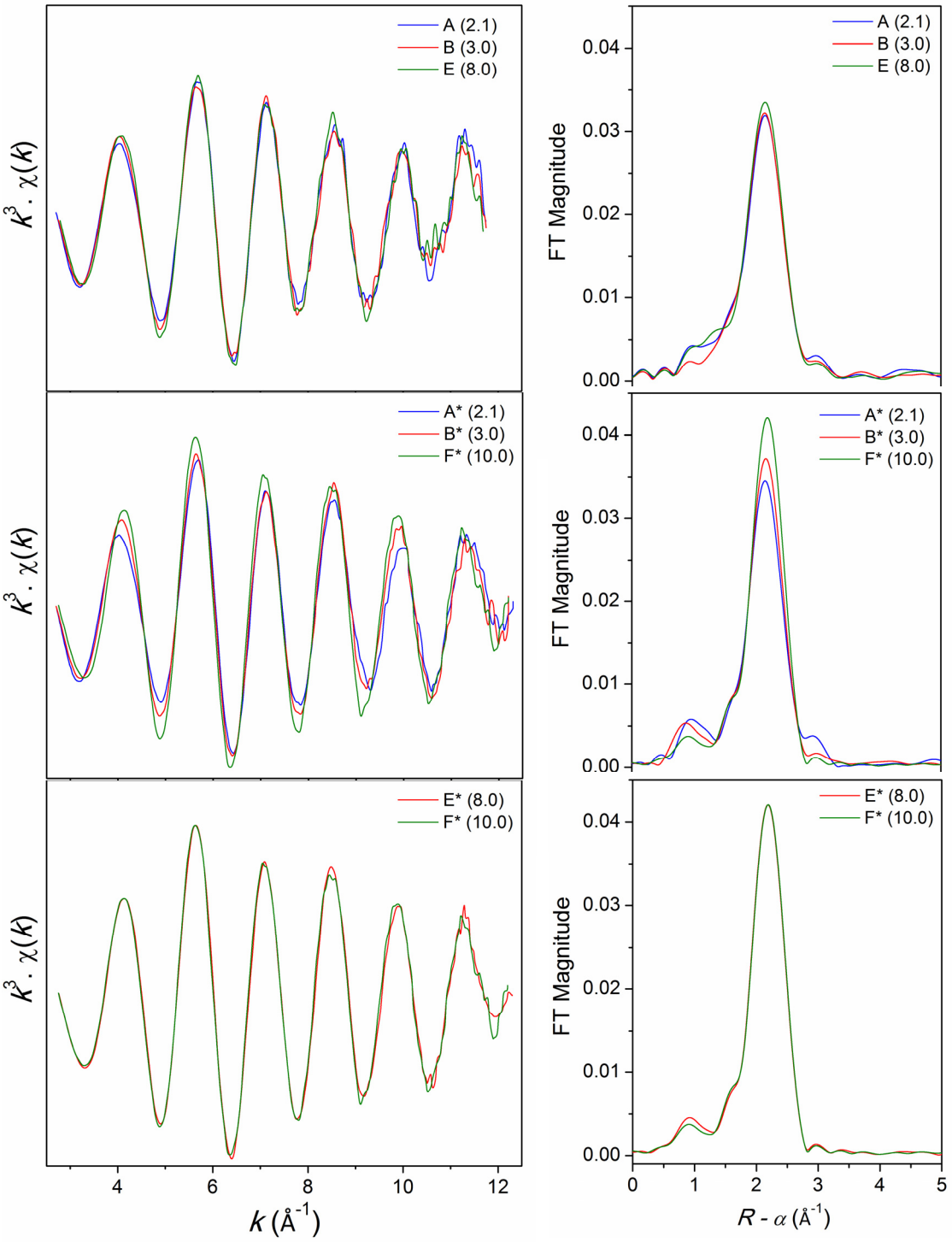

Figure S-8. Pb L_{III}-edge k^3-weighted EXFAS oscillations, and the corresponding Fourier-transforms, compared for Pb(II)-cysteine alkaline solutions A – E ($C_{Pb(II)}$ = 10 mM), and A* – F* ($C_{Pb(II)}$ = 100 mM). The H_2Cys/Pb(II) mole ratios are shown in brackets.

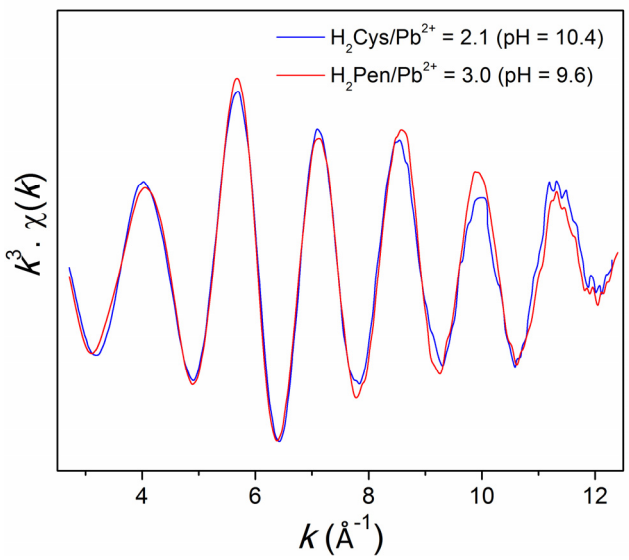

Figure S-9. Comparison between k^3-weighted Pb L_{III}-edge EXAFS spectra of the lead(II) cysteine aqueous solution A* ($C_{Pb(II)}$ = 100 mM, C_{H2Cys} = 210 mM, pH = 10.4), and that of a Pb(II) penicillamine solution ($C_{Pb(II)}$ = 100 mM, C_{H2Pen} = 300 mM, pH = 9.6) with [Pb(*S,N,O*-Pen)(*S*-H_nPen)]$^{2-n}$ (n = 0 - 1) as the dominating species [26].

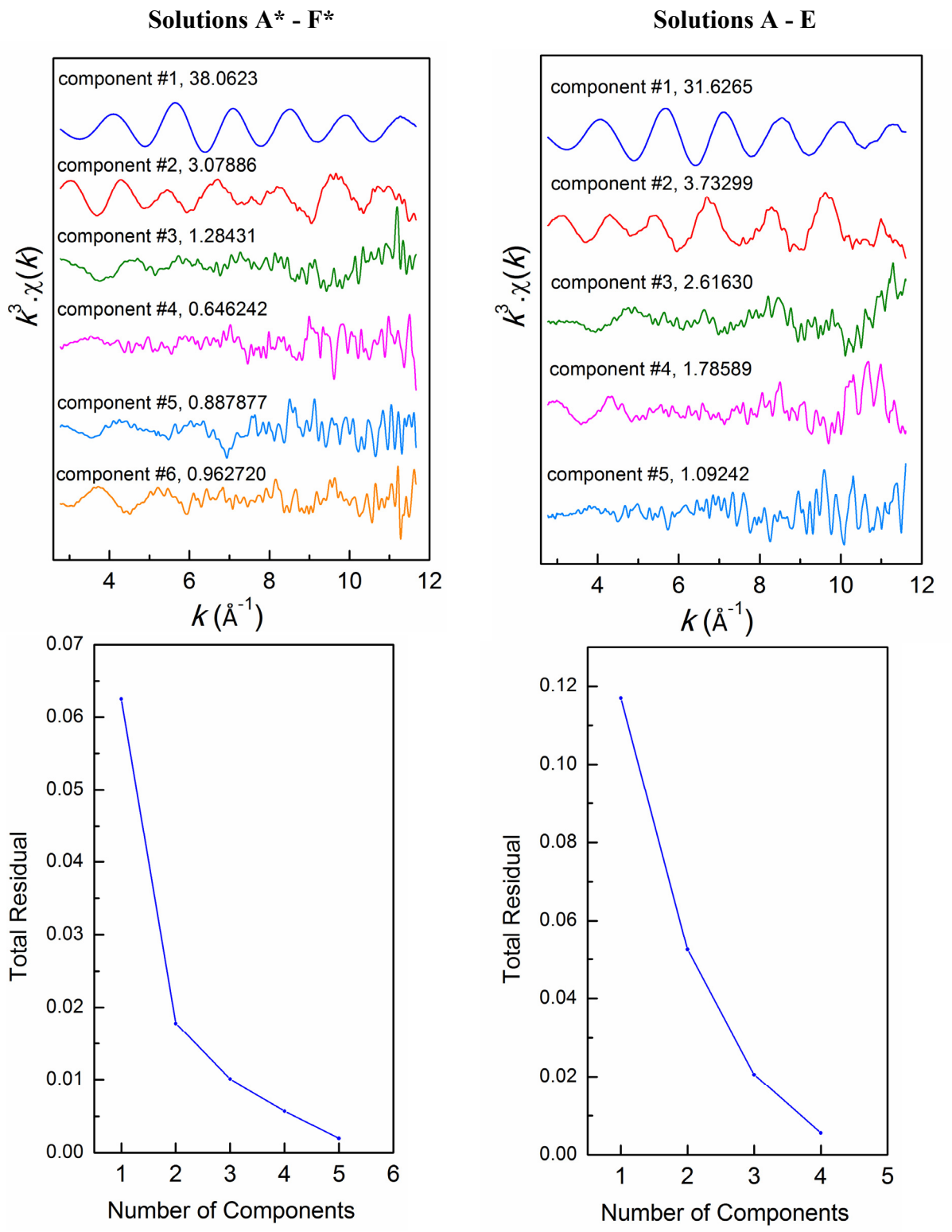

Figure S-10. (*Top*) Principal Component Analysis (PCA) of k^3-weighted, raw experimental EXAFS spectra of Pb(II) cysteine solutions A* - F* and A – E (for compositions, see Table 1), showing all the components and their corresponding eigenvalues. (*Bottom*) Total residual in the reconstructed spectra as a function of the number of components.

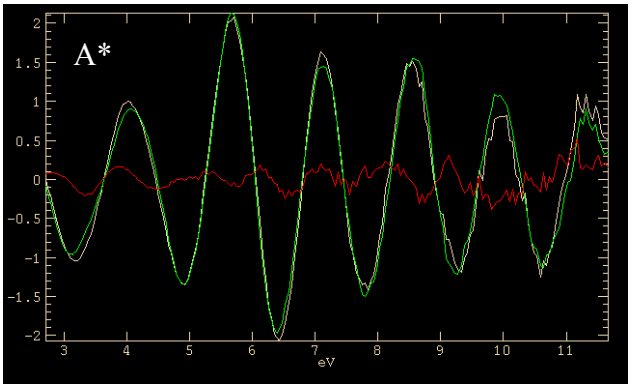

PbS_3	$PbS_2NO + PbS_2N_2$	Residual
3%	97%	0.0211

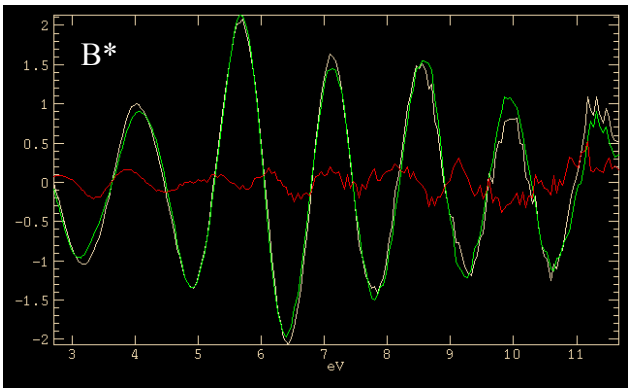

PbS_3	$PbS_2NO + PbS_2N_2$	Residual
11%	89%	0.0267

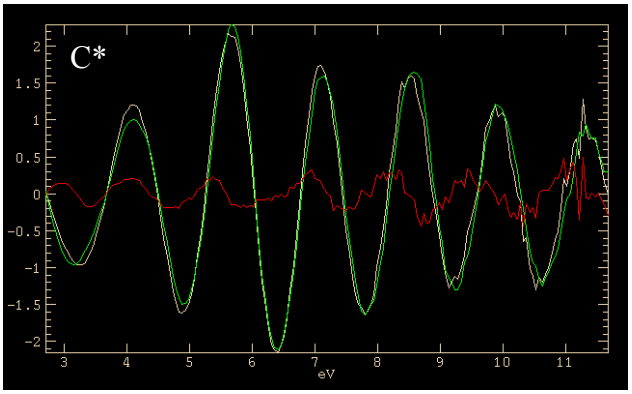

PbS_3	$PbS_2NO + PbS_2N_2$	Residual
15%	85%	0.0330

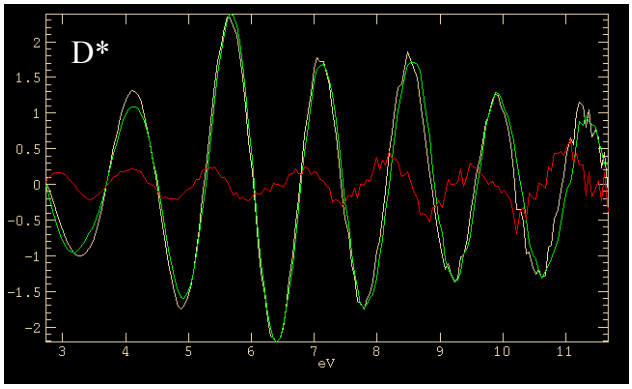

PbS_3	$PbS_2NO + PbS_2N_2$	Residual
25%	75%	0.0469

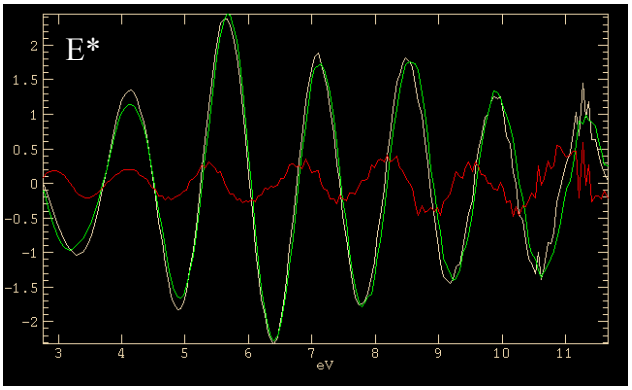

PbS_3	$PbS_2NO + PbS_2N_2$	Residual
30%	70%	0.0531

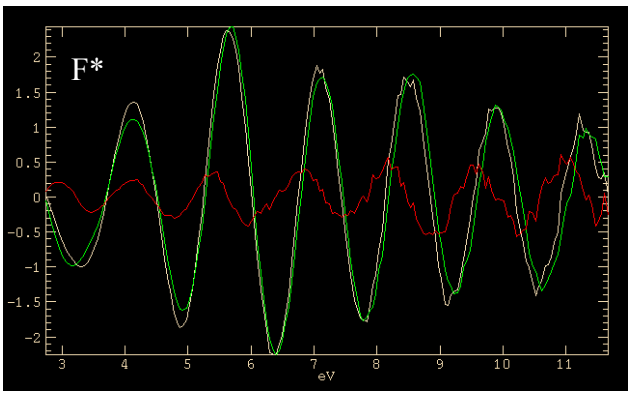

PbS_3	$PbS_2NO + PbS_2N_2$	Residual
25%	75%	0.0761

Figure S-11a. Linear combination of EXAFS oscillations for $PbS_2N(N/O)$ and PbS_3 models fitted (green) to the EXAFS spectra of Pb(II) cysteine solutions A* - F* (white) in *k*-range 2.7 – 11.7 $Å^{-1}$; residual is shown in red.

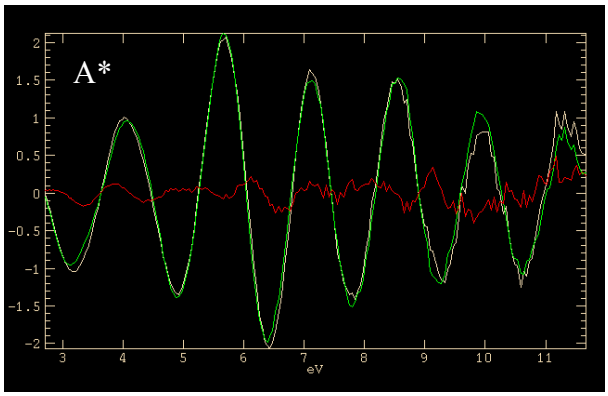

PbS_3N	$PbS_2NO + PbS_2N_2$	Residual
9%	91%	0.0193

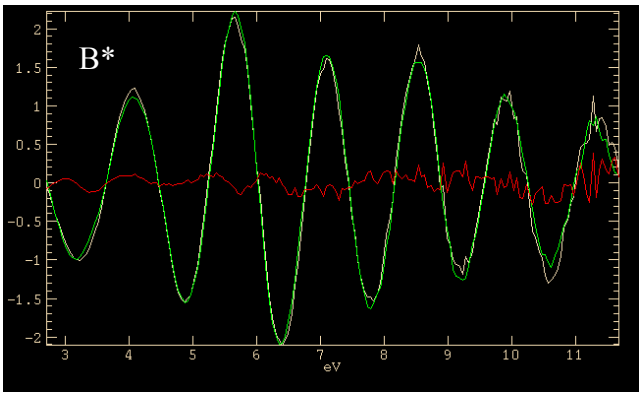

PbS_3N	$PbS_2NO + PbS_2N_2$	Residual
23%	77%	0.0139

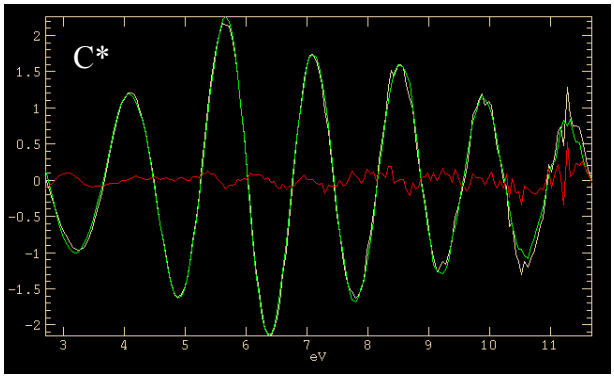

PbS_3N	$PbS_2NO + PbS_2N_2$	Residual
31%	69%	0.0106

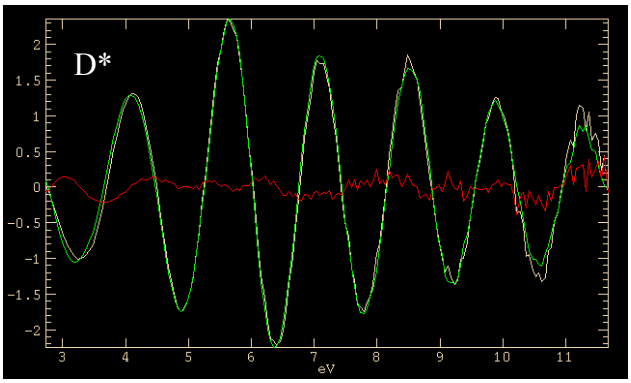

PbS_3N	$PbS_2NO + PbS_2N_2$	Residual
37%	63%	0.0169

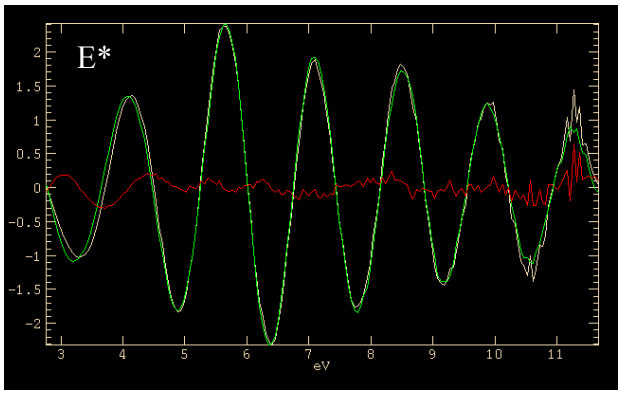

PbS_3N	$PbS_2NO + PbS_2N_2$	Residual
40%	60%	0.0182

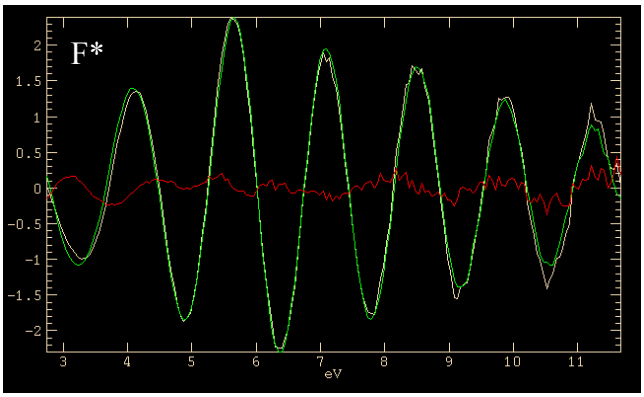

PbS_3N	$PbS_2NO + PbS_2N_2$	Residual
49%	51%	0.0166

Figure S-11b. Linear combination of EXAFS oscillations for PbS_2N(N/O) and PbS_3N models fitted (green) to the EXAFS spectra of Pb(II) cysteine solutions A* - F* (white) in *k*-range 2.7 – 11.7 $Å^{-1}$; residual is shown in red. Estimated error limit for the percentages obtained is ± 10-15%.

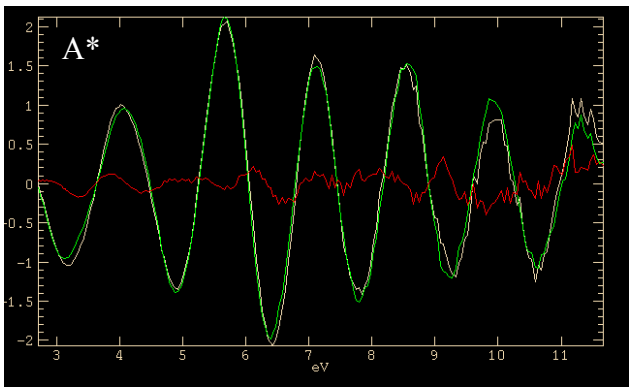

PbS_3N	PbS_3	$PbS_2NO + PbS_2N_2$	Residual
9%	0%	91%	0.0193

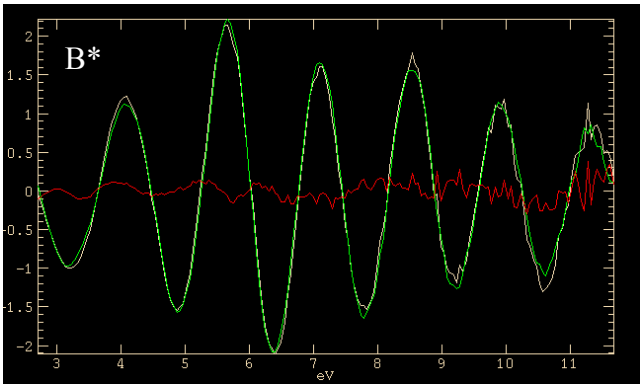

PbS_3N	PbS_3	$PbS_2NO + PbS_2N_2$	Residual
23%	4%	73%	0.0136

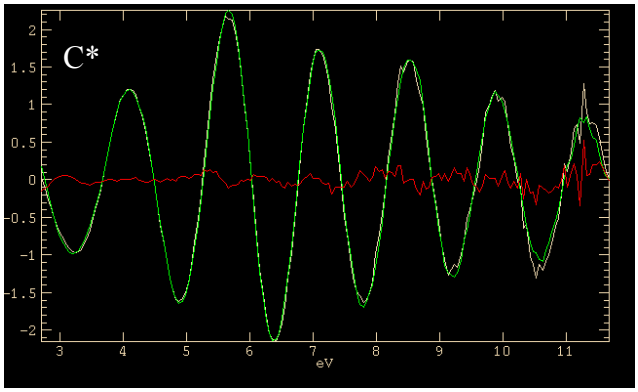

PbS_3N	PbS_3	$PbS_2NO + PbS_2N_2$	Residual
31%	6%	63%	0.0102

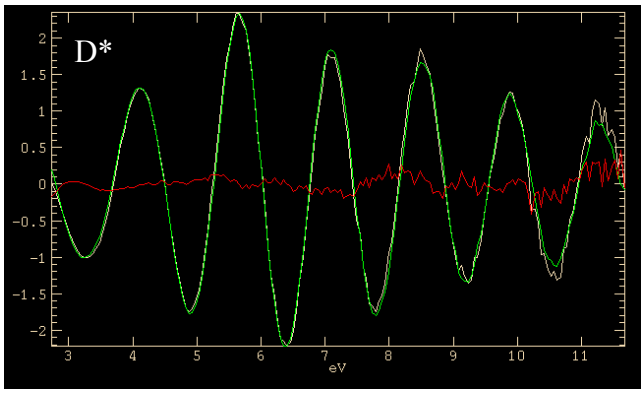

PbS_3N	PbS_3	$PbS_2NO + PbS_2N_2$	Residual
37%	15%	48%	0.0139

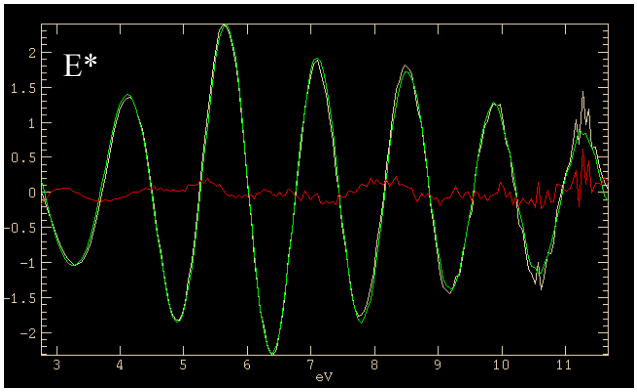

PbS_3N	PbS_3	$PbS_2NO + PbS_2N_2$	Residual
43%	18%	39%	0.0132

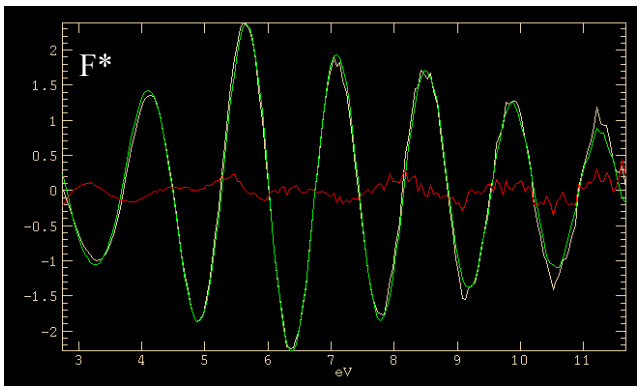

PbS_3N	PbS_3	$PbS_2NO + PbS_2N_2$	Residual
50%	10%	40%	0.0152

Figure S-11c. Linear combination of EXAFS oscillations for PbS_2N(N/O), PbS_3 and PbS_3N models fitted (green) to the EXAFS spectra of Pb(II) cysteine solutions A* - F* (white) in *k*-range 2.7 – 11.7 $Å^{-1}$; residual is shown in red.

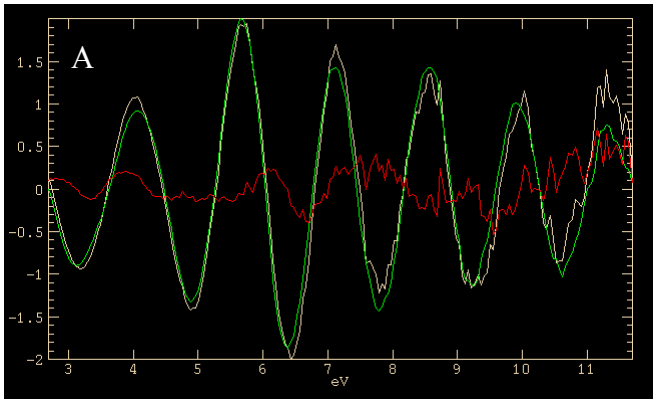

PbS_3N	$PbS_2NO + PbS_2N_2$	Residual
11%	89%	0.0460

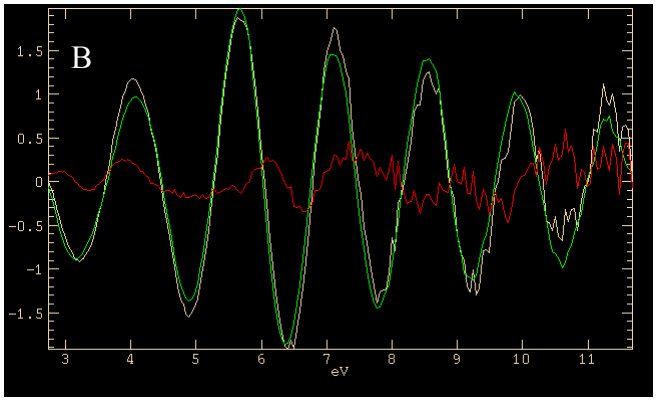

PbS_3N	$PbS_2NO + PbS_2N_2$	Residual
20%	80%	0.0393

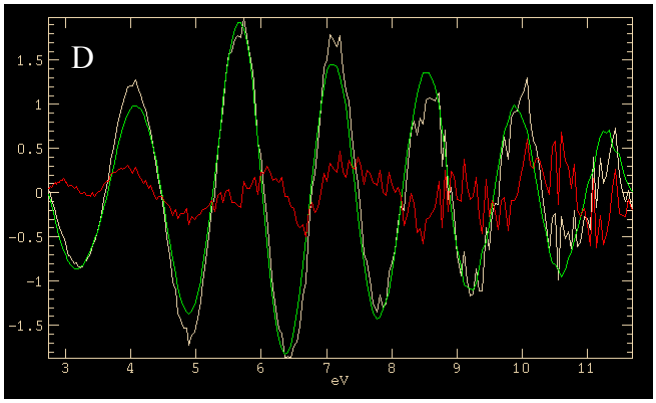

PbS_3N	$PbS_2NO + PbS_2N_2$	Residual
26%	74%	0.0559

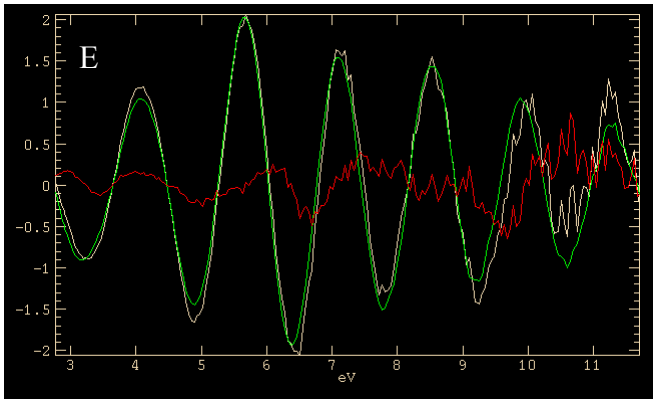

PbS_3N	$PbS_2NO + PbS_2N_2$	Residual
27%	73%	0.0549

Figure S-11d. Linear combination of EXAFS oscillations for PbS_2N(N/O) and PbS_3N models fitted (green) to the EXAFS spectra of Pb(II) cysteine solutions A - E (white) in *k*-range 2.7 – 11.7 $Å^{-1}$; residual is shown in red. Estimated error limit for the percentages obtained is ± 10-15%.

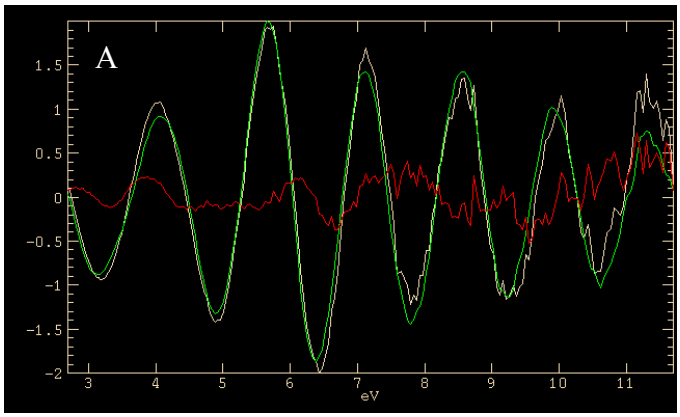

PbS_3N	PbS_3	$PbS_2NO + PbS_2N_2$	Residual
10%	4%	86%	0.0458

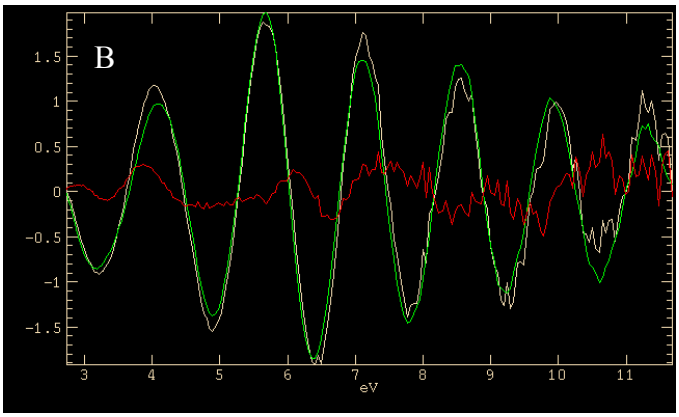

PbS_3N	PbS_3	$PbS_2NO + PbS_2N_2$	Residual
18%	8%	74%	0.0385

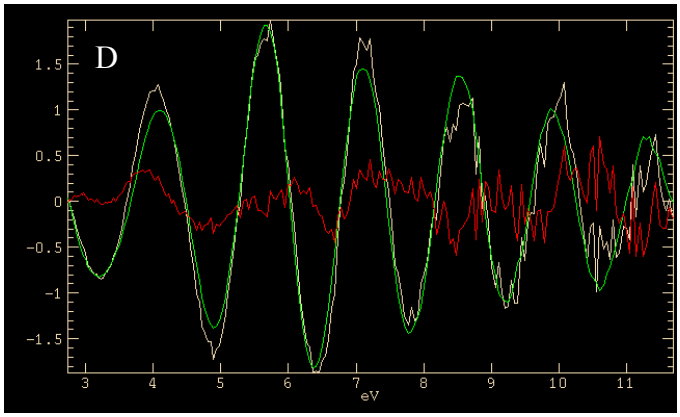

PbS_3N	PbS_3	$PbS_2NO + PbS_2N_2$	Residual
23%	12%	65%	0.0543

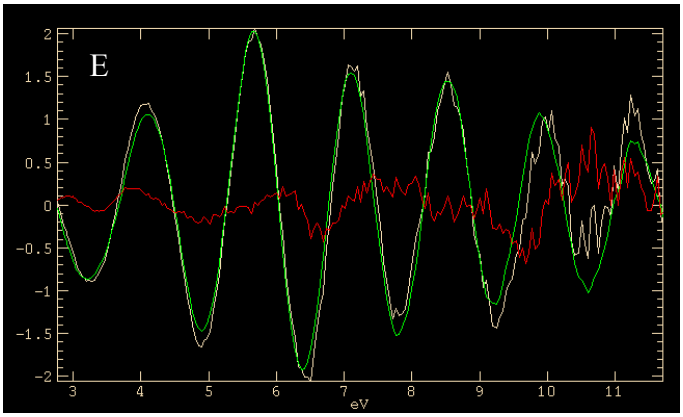

PbS_3N	PbS_3	$PbS_2NO + PbS_2N_2$	Residual
25%	12%	63%	0.0532

Figure S-11e. Linear combination of EXAFS oscillations for $PbS_2N(N/O)$, PbS_3 and PbS_3N models fitted (green) to the EXAFS spectra of Pb(II) cysteine solutions A - E (white) in *k*-range 2.7 – 11.7 $Å^{-1}$; residual is shown in red.

Table S-3. Results of fitting the raw, k^3-weighted Pb L_{III}-edge EXAFS spectra of Pb(II) cysteine solutions A* - F* and A – E with linear combinations of EXAFS oscillations for $PbS_2N(N/O)$, PbS_3N and PbS_3 models (see Figures S-11c and S-11e). [a]

Solution (H_2Cys/Pb^{II} mole ratio)	$\delta(^{207}Pb)$ ppm	$PbS_2NO + PbS_2N_2$ (%)	PbS_3N (%)	PbS_3 (%)
A (2.1)	2006	86	10	4
B (3.0)	2112	74	18	8
D (5.0)	2229	65	23	12
E (8.0)	2310	63	25	12
A* (2.0)	2010	91	9	0
B* (3.0)	2219	73	23	4
C* (4.0)	2316	63	31	6
D* (5.0)	2350	48	37	15
E* (8.0)	2418	39	43	18
F* (10.0)	2507	40	50	10

[a] Raw k^3-weighted EXAFS spectra of 0.1 M lead(II) solutions containing penicillamine (C_{H2Pen} = 0.3 M; pH = 9.6), or *N*-acetylcysteine (C_{H2NAC} = 1.0 M, pH = 9.1) were used for the $PbS_2N(N/O)$ and PbS_3 species, respectively. The EXAFS oscillation for PbS_3N was theoretically simulated (see text). Estimated error limit of the relative amounts is ± 10 – 15%.

Table S-4. Least-squares curve-fitting of the k^3-weighted EXAFS spectra for Pb(II)-cysteine alkaline aqueous solutions A – B ($C_{Pb(II)}$ = 10 mM) and A*, B* and F* ($C_{Pb(II)}$ = 100 mM), containing different H_2Cys/ Pb(II) mole ratios (Table 1), using different fitting models. [a]

		Pb-(N/O)			Pb-S				
Solution	Model	*N*	*R* (Å)	σ^2 (Å^2)	*N*	*R* (Å)	σ^2 (Å^2)	ΔE_0	$\Re$ [b]
A	**I**	2*f*	2.410	0.0206	2*f*	2.638	0.0058	-1.1	20.0
	II	2*f*	2.400	0.0143	1.6	2.641	0.0043	-0.9	19.5 *
B	**I**	2*f*	2.431	0.0170	2*f*	2.643	0.0062	-0.1	14.0
	II	2*f*	2.430	0.0165	2.0	2.644	0.0061	-0.1	14.0 *

		Pb-(N/O)			Pb-S				
Solution	Model	*N*	*R* (Å)	σ^2 (Å^2)	*N*	*R* (Å)	σ^2 (Å^2)	ΔE_0	$\Re$ [b]
A*	**I**	2*f*	2.417	0.0199	2*f*	2.639	0.0055	-1.4	22.0
	II	2*f*	2.416	0.0201	2.0	2.639	0.0055	-1.4	22.0 *
	III	1*f*	2.335	0.0081	2*f*	2.636	0.0055	-1.2	21.9
		1*f*	2.503	0.0081[c]					
B*	**I**	2*f*	2.425	0.0177	2*f*	2.652	0.0050	0	18.2
	II	2*f*	2.429	0.0237	2.3	2.649	0.0059	-0.4	18.0 *
	III	1*f*	2.332	0.0143	2*f*	2.649	0.0050	-0.3	18.1
		1*f*	2.496	0.0143[c]					
F*	**IV**	1.5*f*	2.452	0.0290	2.9	2.662	0.0064	1.1	12.9
	V [d]	1.5*f*	2.429	0.0185	2.5*f*	2.663	0.0055	1.2	13.0*
	VI	1*f*	2.391	0.0200	2.8	2.661	0.0062	0.4	12.9
	VII [e]	1*f*	2.403	0.0134	2.5*f*	2.662	0.0054	0.7	13.0

[a] S_0^2 = 0.9 fixed (obtained from fitting the EXAFS spectrum of solid PbPen) [33]; *k*-range = 2.7 – 11.7 Å^{-1}; *f* = fixed value; *R* ± 0.04 Å; σ^2 ± 0.002 Å^2; [b] The residual (%) from the least-squares curve fitting is defined as:

$$\frac{\sum_{i=1}^{N} | y_{exp}(i) - y_{theo}(i)|}{\sum_{i=1}^{N} | y_{exp}(i)|} \text{ X } 100$$

where y_{exp} and y_{theo} are experimental and theoretical data points, respectively; [c] correlated; [d] assuming a 50:50% mixture of PbS_2N(N/O) and PbS_3N coordination environments; [e] assuming a 50:50% mixture of PbS_2N(N/O) and PbS_3 coordination. * Selected model for Table 4 and Figure 6.

Table S-5. Least-squares curve-fitting of the k^3-weighted EXAFS spectra for crystalline $Pb(aet)_2$ [a]

Model	Path	N	R (Å)	σ^2 (Å^2)	S_0^2	ΔE_0	$\Re$
I	Pb-(N/O)	2*f*	2.538	0.0040	0.9 *f* [b]	3.5	20.7
	Pt-S	2*f*	2.632	0.0069			
	Pt-C	4*f*	3.437	0.0156			
II	Pb-(N/O)	2*f*	2.532	0.0020	0.9 *f* [b]	1.9	20.0
	Pt-S [c]	2.8	2.615	0.0099			
	Pt-C	4*f*	3.406	0.0158			
III	Pb-(N/O)	2*f*	2.540	0.0033	1.0 *f*	3.3	20.4
	Pt-S	2*f*	2.623	0.0078			
	Pt-C	4*f*	3.437	0.0174			

[a] Mixed 50:50 (w/w) with boron nitride; $Pb(aet)_2$ crystal structure [25] was used as FEFF model; k-range = 2.7 – 12.4 Å^{-1}; f = fixed; $R \pm 0.04$ Å; $\sigma^2 \pm 0.002$ Å^2 ; [b] $S_0^2 = 0.9$ fixed (obtained from fitting EXAFS spectrum of solid PbPen) [33]. [c] Simultaneous refinement of coordination number and σ^2 for the Pb-S path shows the strong correlation between these parameters, which contribute in the EXAFS amplitude.

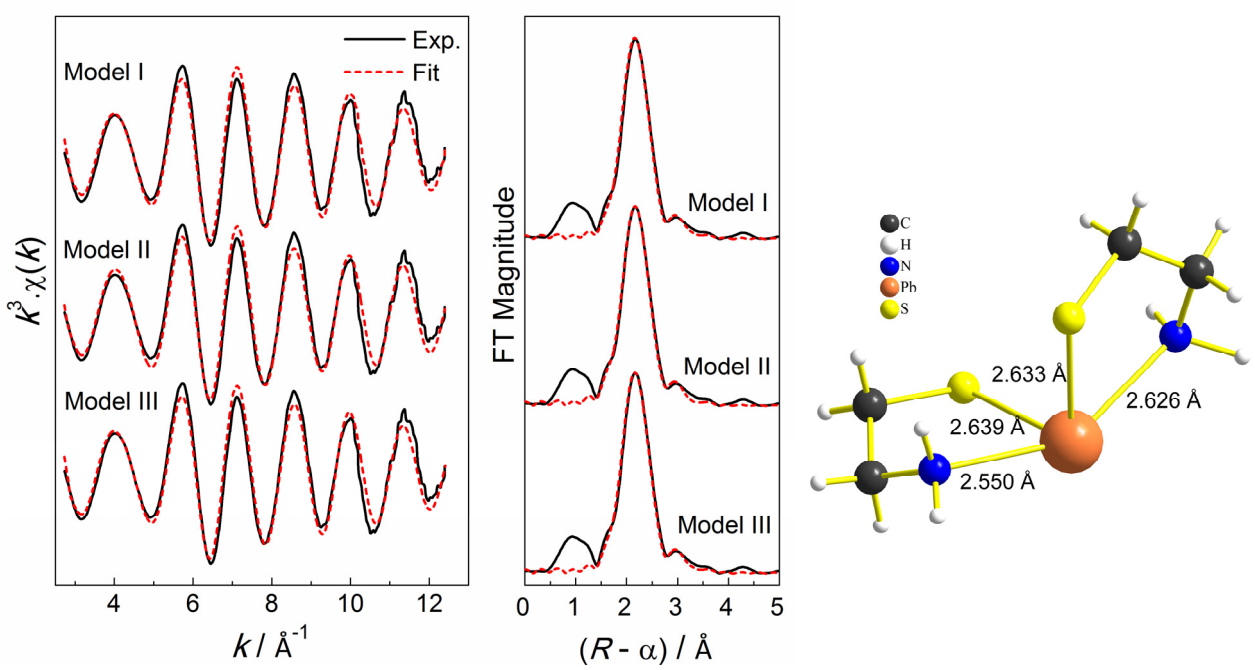

Figure S-12. EXAFS fitting results for crystalline $Pb(aet)_2$ (see Table S-5); structure from *Ref.* 25

Table S-6. Survey of Pb(II) complexes with PbS_3N coordination in CSD version 5.35 (Nov 2013)

	CSD Code	*Pb-S (Å)*	*Pb-N (Å)*	**Reference**
1	XIRBUW	2.626 2.664 3.174	2.571	G.G. Briand, A.D. Smith, G. Schatte, A.J. Rossini, R.W. Schurko *Inorg. Chem.* **2007***, 46*, 8625
2	XIRCAD	2.618 2.648 3.267	2.497	G.G. Briand, A.D. Smith, G. Schatte, A.J. Rossini, R.W. Schurko *Inorg. Chem.* **2007***, 46*, 8625
3	PAQVOT	2.704 2.892 3.086	2.411	M. S. Bharara; C. H. Kim; S. Parkin; D.A. Atwood *Polyhedron* **2005,** *24*, 865-871
	Pb-X Range	2.618 – 3.267	2.411 – 2.571	
	Average	2.853	2.493	